Electronic Supplementary Material (ESI) for Journal of Materials Chemistry A.

Supplementary Information

Rational Design of Free-Standing 3D Porous MXene/RGO Hybrid Aerogels as Polysulfides Reservoir for Stable Lithium-Sulfur Batteries

Jianjun Song,[a,b] Xin Guo,[b] Jinqiang Zhang,[b] Yi Chen,[b] Chaoyue Zhang,[b] Linqu Luo,[a] Fengyun Wang,[*a] and Guoxiu Wang[*b]

[a]*State Key Laboratory of Bio-Fibers and Eco-Textiles and College of Physics, Qingdao University, Qingdao 266071, P.R China. Email: fywang@qdu.edu.cn*

[b]*Centre for Clean Energy Technology, Faculty of Science, University of Technology Sydney, Sydney, New South Wales 2007, Australia. Email: Guoxiu.Wang@uts.edu.au*

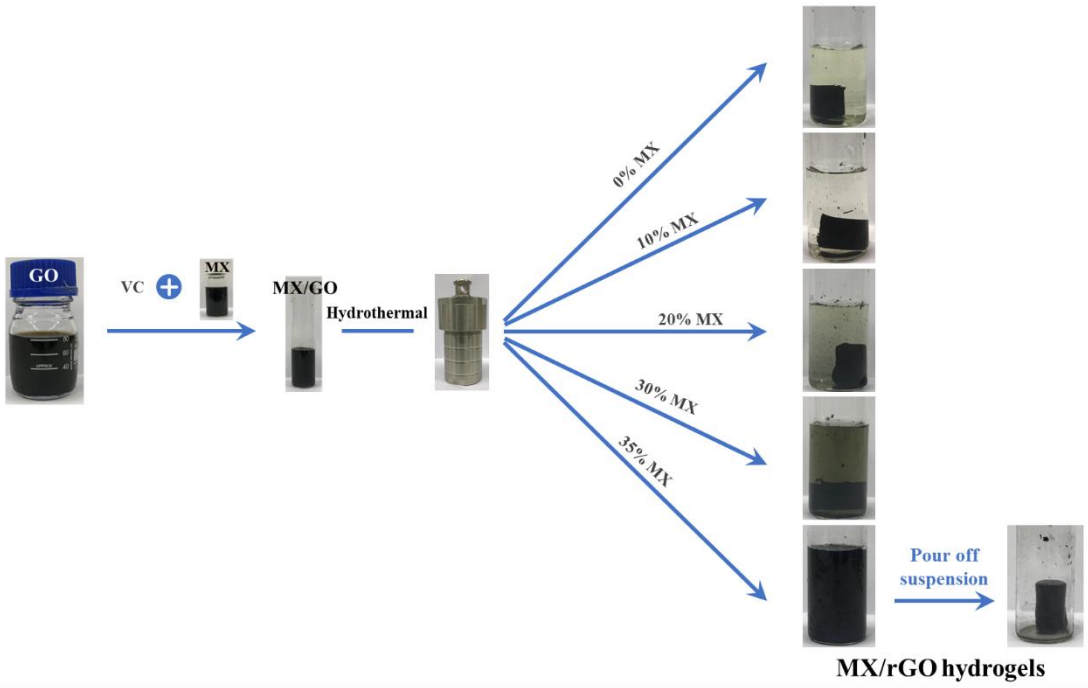

Fig. S1 (a) Photographs of the preparation process of the MX/G hydrogels with different ratios of MXene.

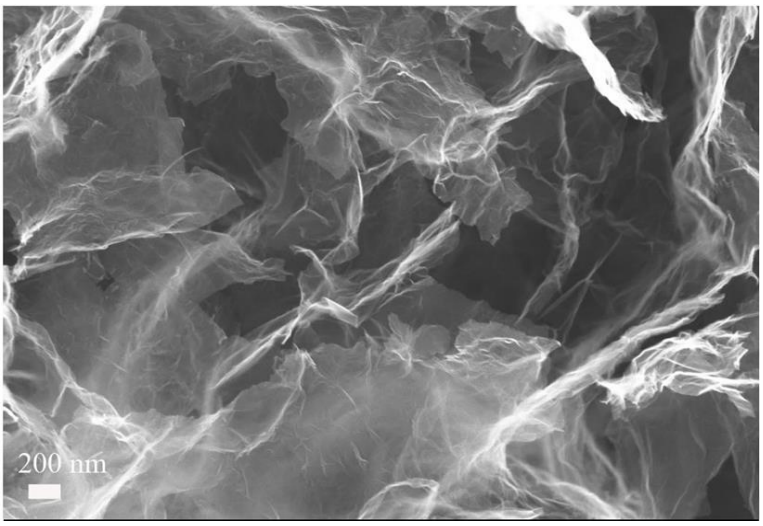

Fig. S2 SEM images of MX/G-30 aerogels.

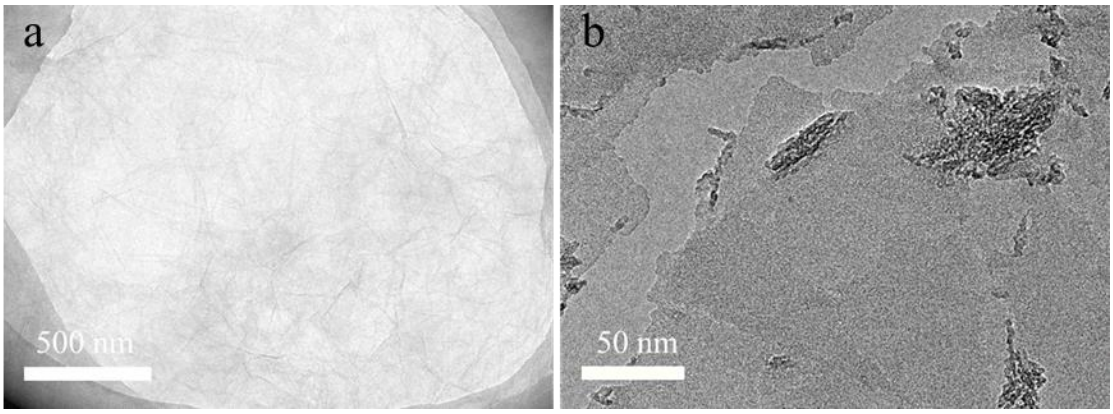

Fig. S3 TEM images of GO (a) and $Ti_3C_2T_x$ MXene (b).

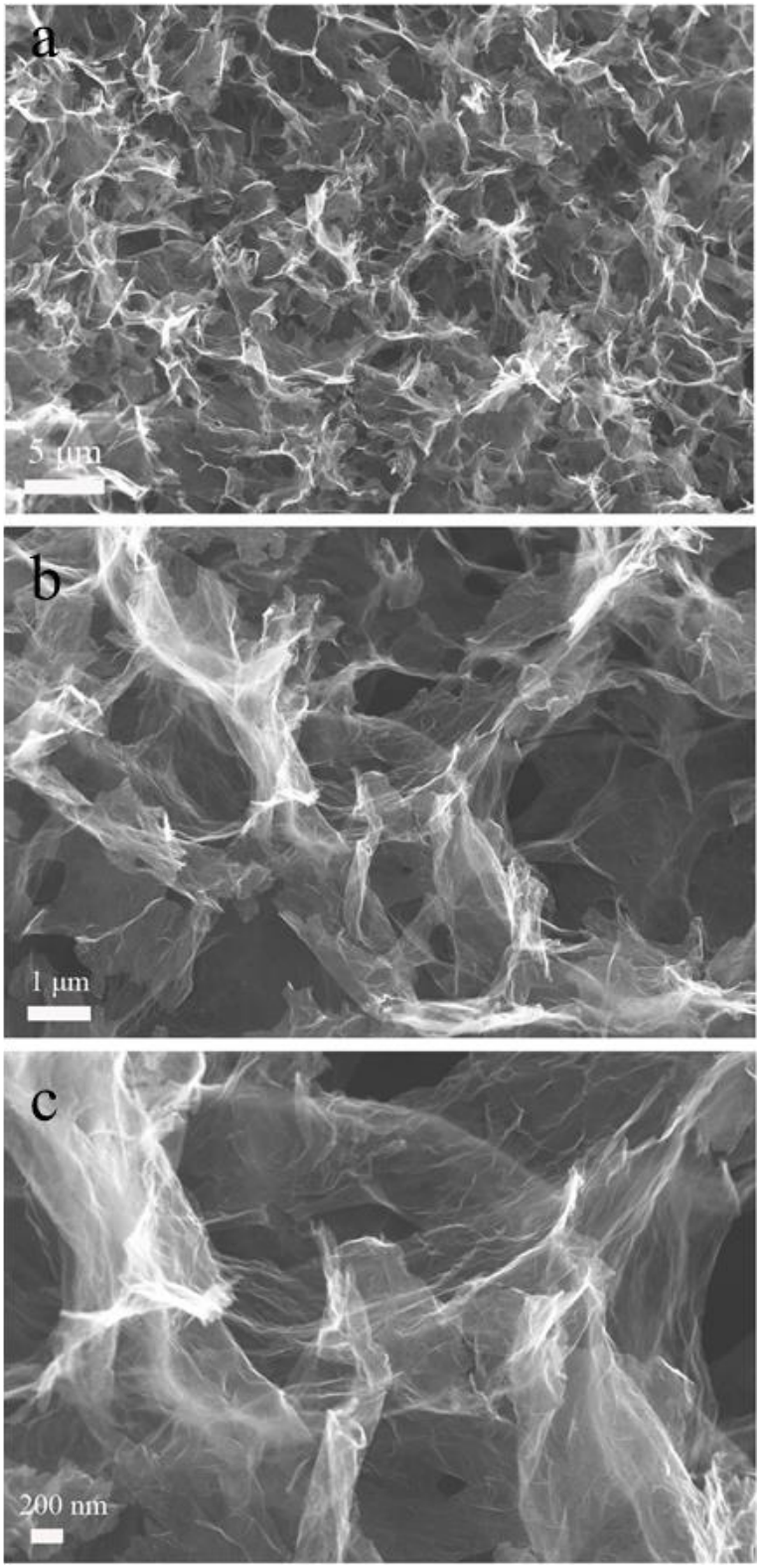

Fig. S4 SEM images of rGO aerogel.

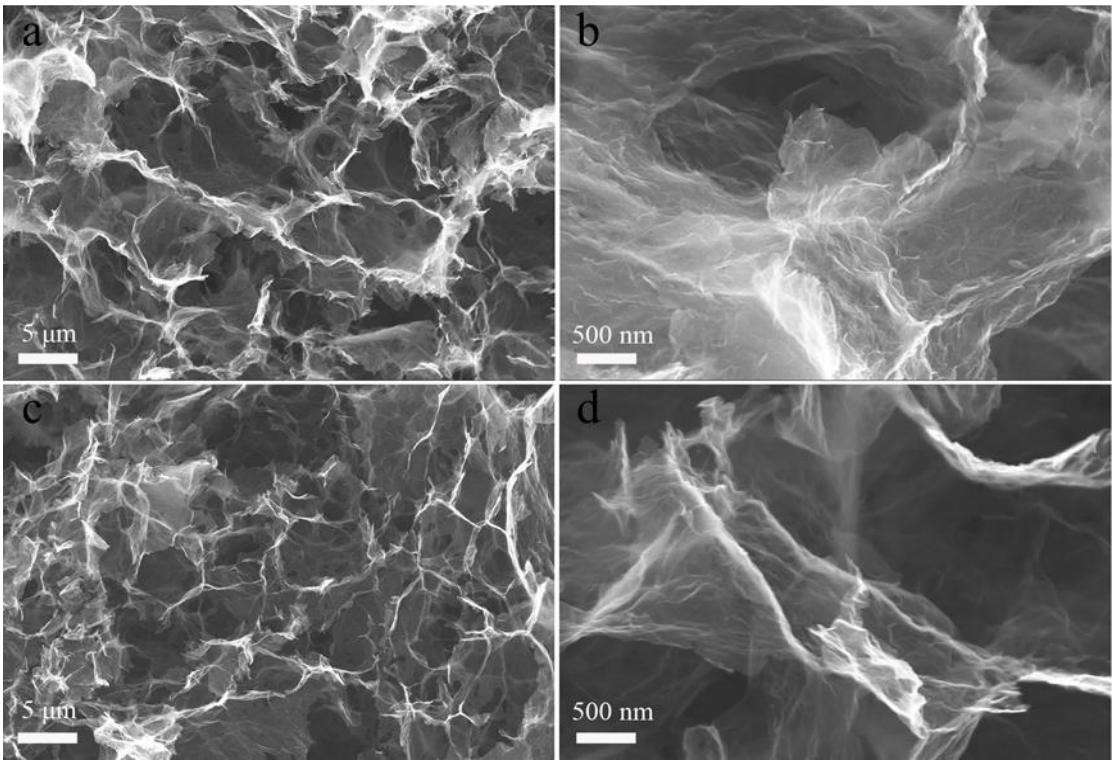

Fig. S5 SEM images of MX/G-10 (a,b) and MX/G-20 (c,d) aerogels.

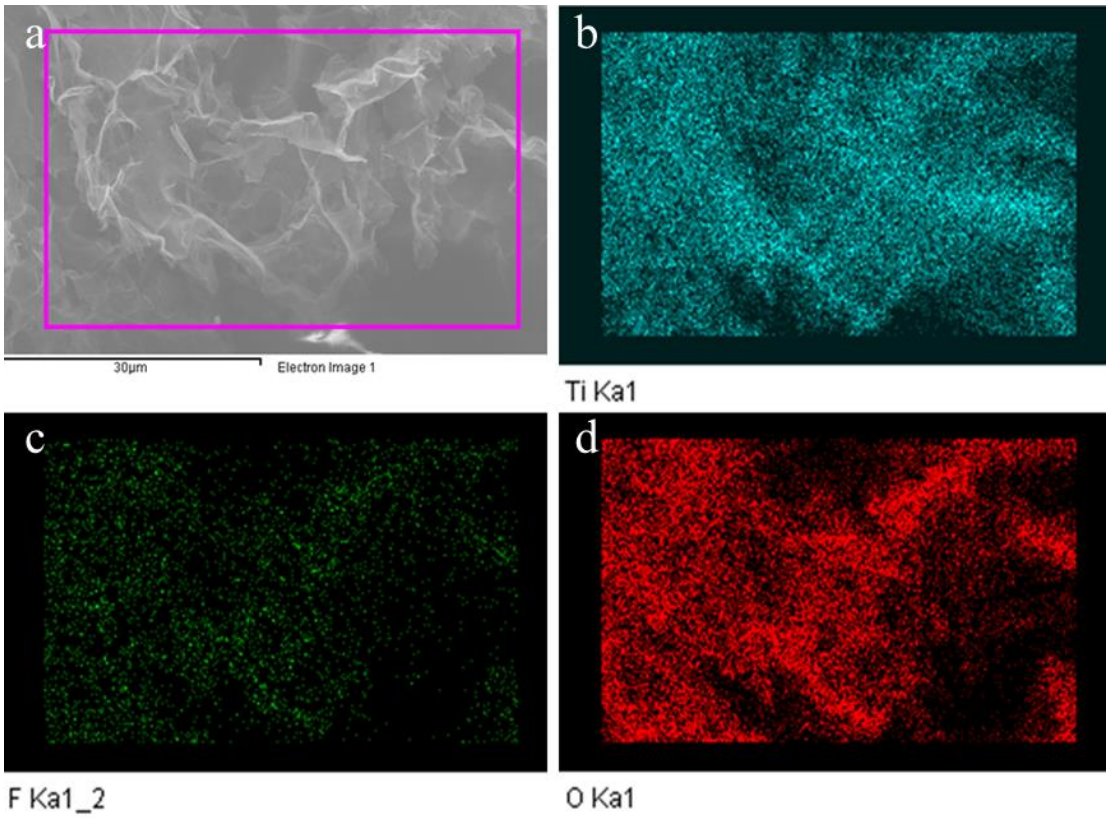

Fig. S6 SEM image and EDS spectrum mapping: Ti, F and O elemental distribution of MX/G-30 aerogel.

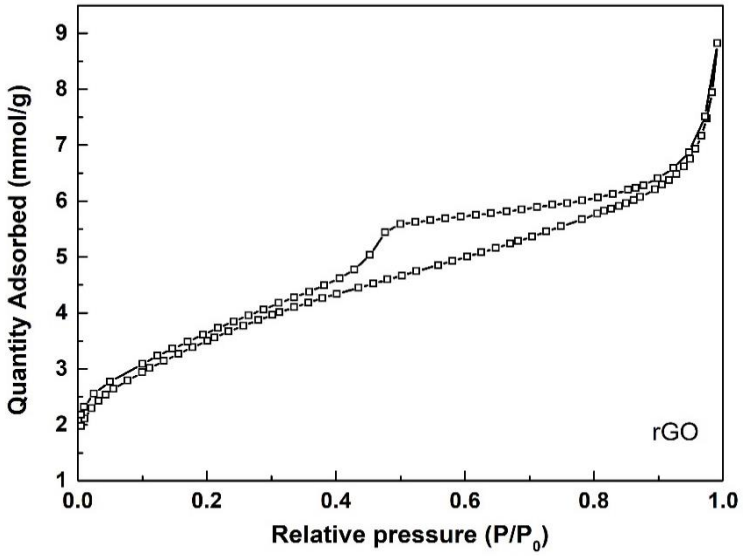

Fig. S7 N_2 isothermal adsorption-desorption isotherms of the rGO aerogel.

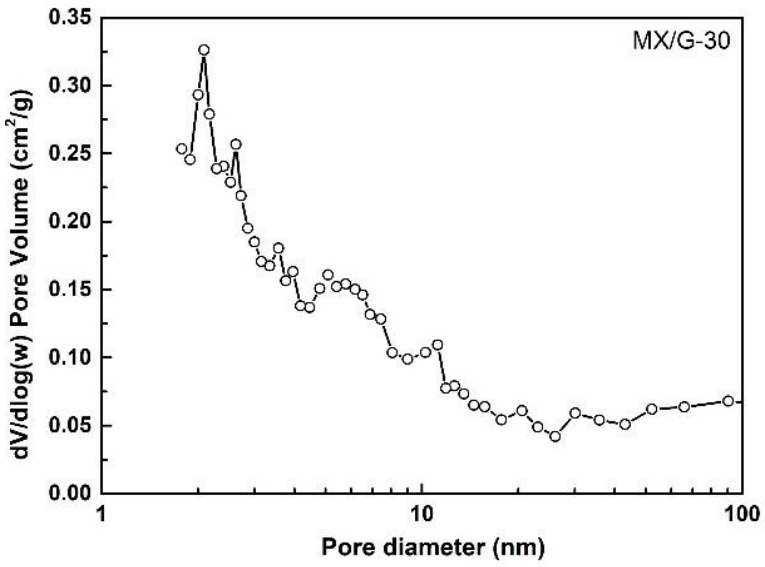

Fig. S8 Pore size distribution of MX/G-30 aerogel.

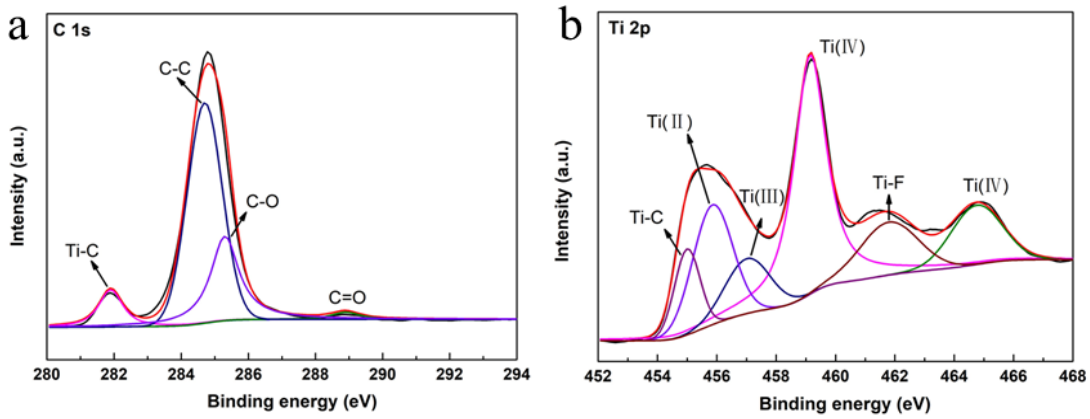

Fig. S9 C 1s (a) and Ti 2p (b) XPS spectrum of the pure $Ti_3C_2T_x$ MXene.

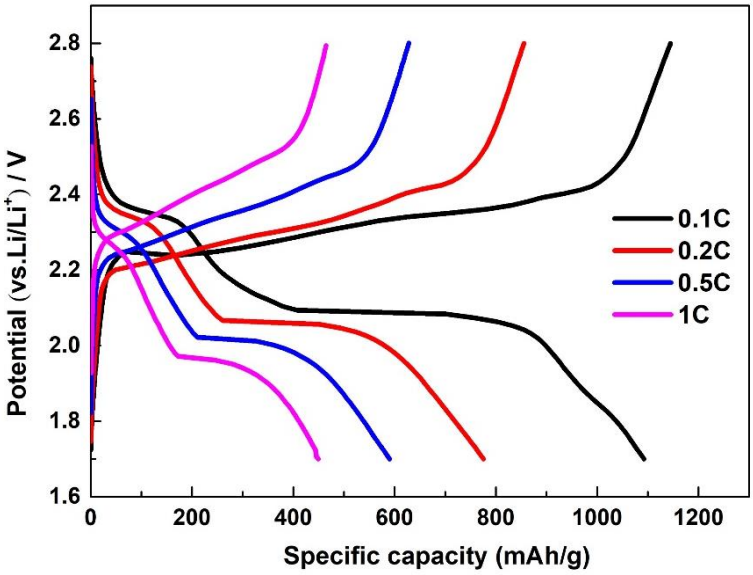

Fig. S10 First charge/discharge curves of Li-S cell with the rGO electrode at various rates.

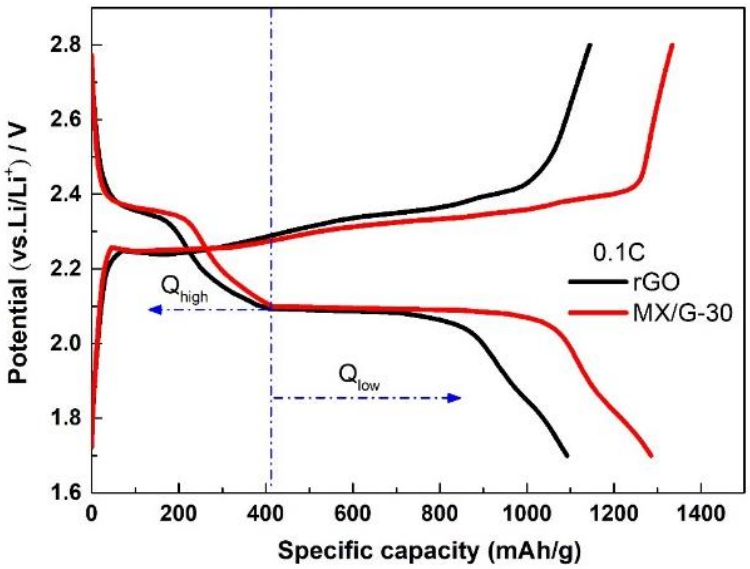

Fig. S11 Comparison of first charge/discharge curves of Li-S cell with the rGO and MX/G-30 electrodes at 0.1 C rate.

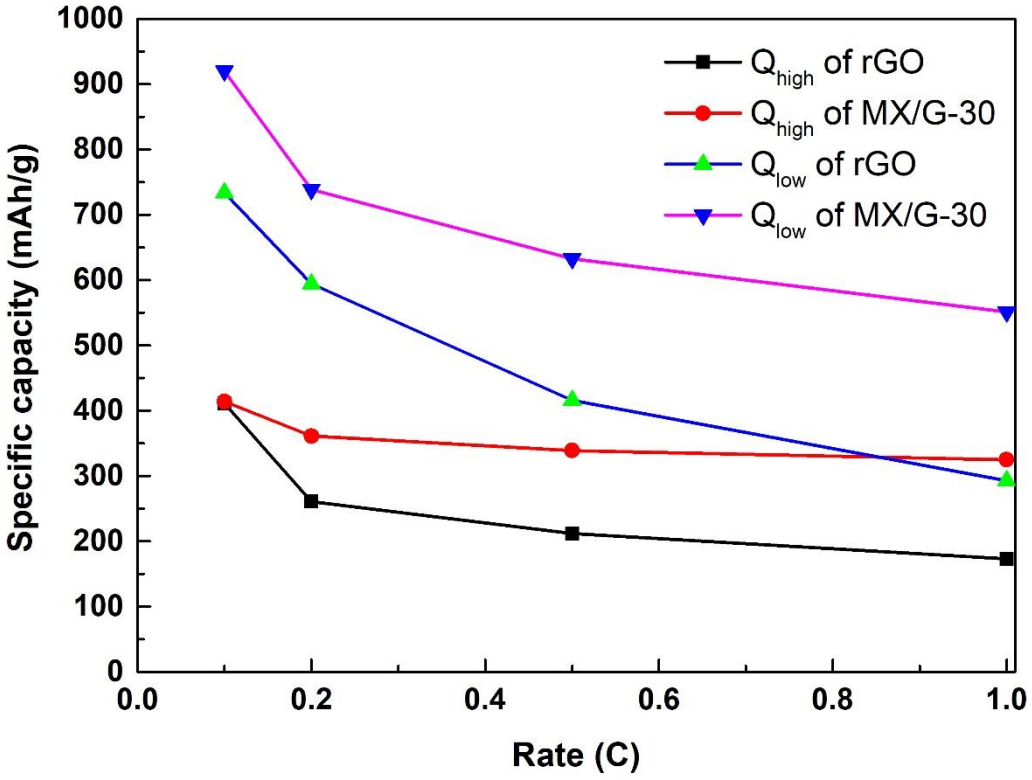

Fig. S12 Q_{high} and Q_{low} of Li-S cell with the rGO and MX/G-30 electrodes at different rates.

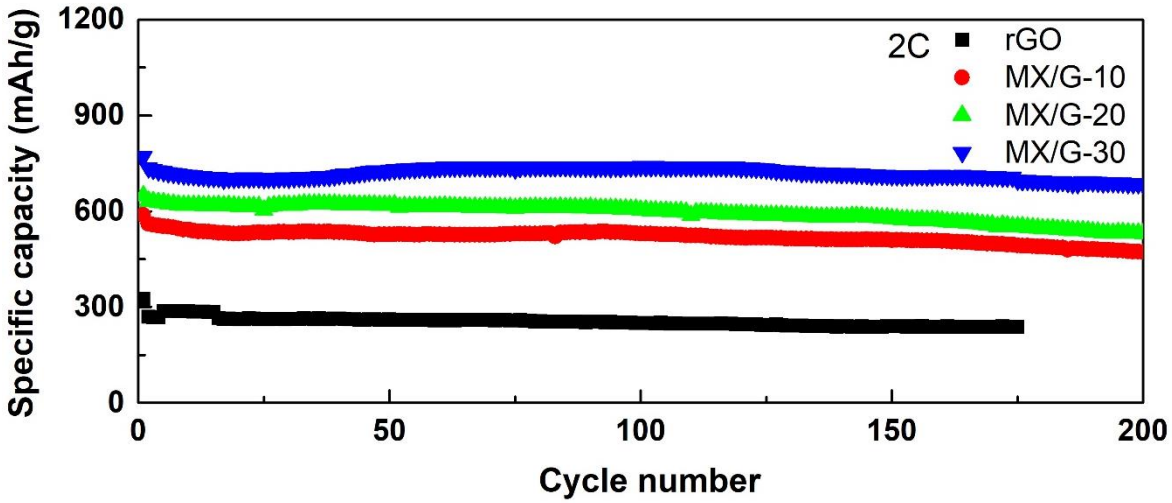

Fig. S13 Cycling performance of the Li-S cells with rGO, MX/G-10, MX/G-20, and MX/G-30 electrodes at 2 C rate after rate capability test.

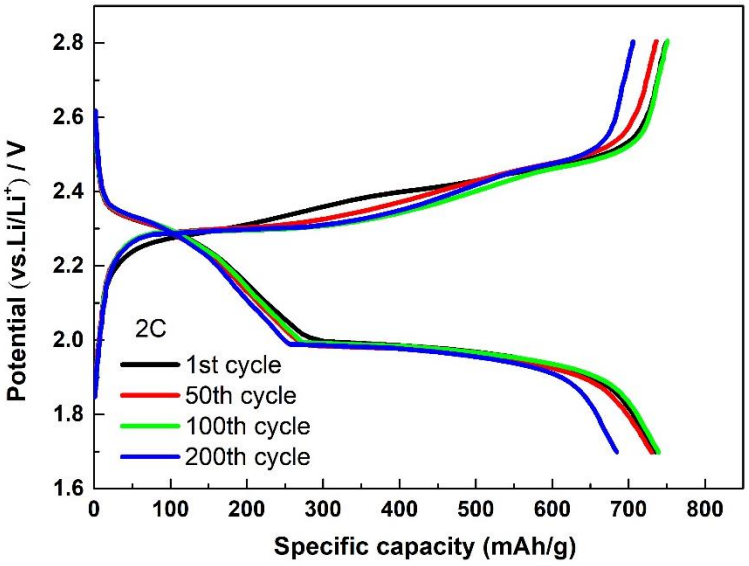

Fig. S14 Charge/discharge curves at 1st, 50th, 100th, and 200th cycles of the Li-S cell with MX/G-30 electrode at 2 C rate.

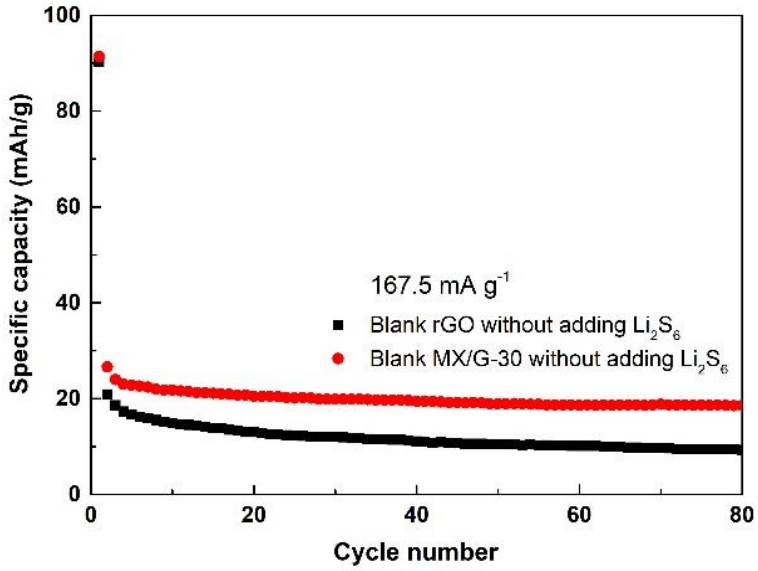

Fig. S15 Cycling stability of the blank rGO and MX/G-30 electrodes in the voltage range of 1.7-2.8 V at a current density of 167 mA g^{-1} for 80 cycles.

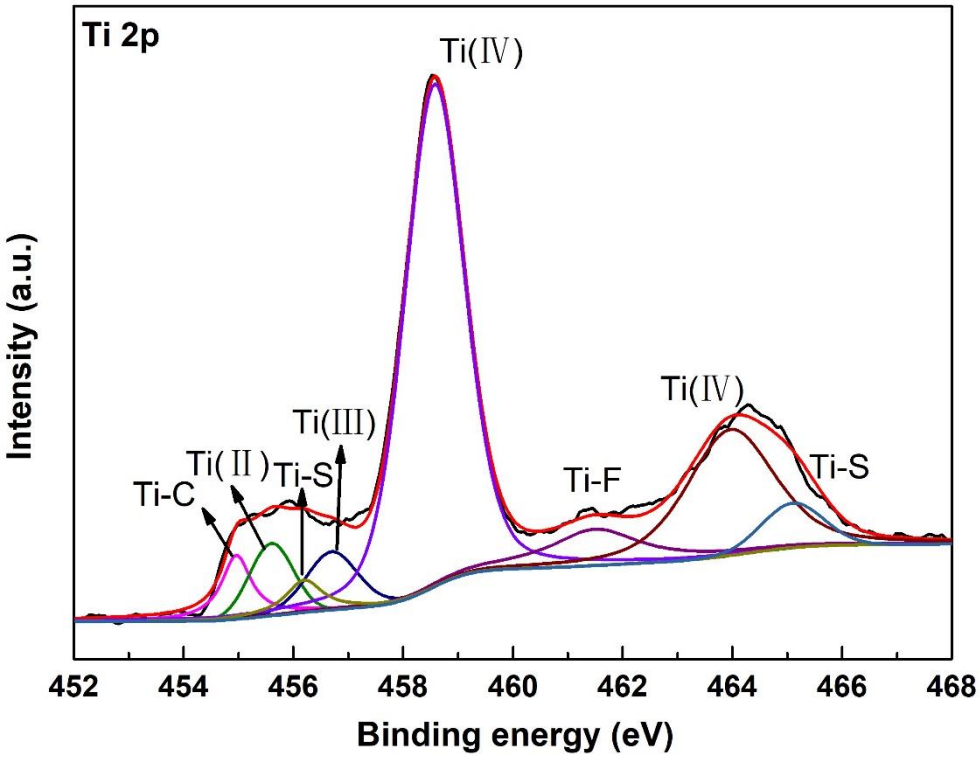

Fig. S16 Ti 2p XPS spectrum of the cycled MX/G-30 electrode.

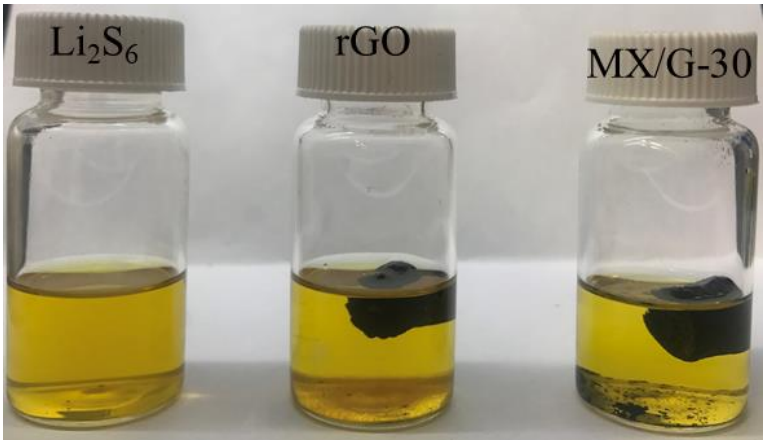

Fig. S17 Initial state of Li_2S_6 adsorption test by soaking 20 mg rGO and MX/G-30 aerogel into 5 mM Li_2S_6 solution. All operations were conducted in the glove box.

Table S1 Comparison of the areal capacity between Li-S batteries employing MXene-based sulfur host.

sulfur host	Sulfur loading (mg cm^{-2})	Rate (C)	Areal capacity (mAh cm^{-2})	Ref.
Ti_2C MXene sheets	1.0	0.5	1.09	S1
Ti_3C_2 MXene Nanosheet/Carbon-Nanotube Composites	1.5	0.2	1.8	S2
	5.5	0.2	5	
Nitrogen-Doped $Ti_3C_2T_x$ MXene Nanosheet	1.5	0.2	1.69	S3
	5.1	0.2	4.2	
Ti_3C_2 Nanoribbon Framework	0.7-1	0.2	0.74-1.06	S4
$Ti_3C_2T_x$ MXene Ink	2.49	0.1	3.36	S5
MXene/rGO Aerogel	6.0	0.1	5.27	This work

References

S1 X. Liang, A. Garsuch and F. Nazar Linda, *Angew. Chem. Int. Ed.*, 2015, **54**, 3907-3911.
S2 L. Xiao, R. Yverick, K. C. Yuen, P. Quan and N. L. F., *Adv. Mater.*, 2017, **29**, 1603040.
S3 W. Bao, L. Liu, C. Wang, S. Choi, D. Wang and G. Wang, *Adv. Energy Mater.*, 2018, **8**, 1702485.
S4 Y. Dong, S. Zheng, J. Qin, X. Zhao, H. Shi, X. Wang, J. Chen and Z.-S. Wu, *ACS Nano*, 2018, **12**, 2381-2388.
S5 H. Tang, W. Li, L. Pan, C.P. Cullen, Y. Liu, A. Pakdel, D. Long, J. Yang, N. Mcevoy, G.S. Duesberg, V. Nicolosi and C. Zhang, *Adv. Sci.*, 2018, **5**, 1800502.